Algorithm for the detection of faults in rolling element bearings running under tacholess and variable rotating speed conditions

Lisa María Valdés[1], Fidel Ernesto Hernández Montero[2], Andy Rodríguez Lorenzo[3]

[1]Technological University of Havana, Cujae, Marti 270, Havana, Cuba
[2]Technological University of Havana, Cujae, Marti 270, Havana, Cuba
fhernandez@tele.cujae.edu.cu
[3]University of Havana, S. Lázaro and L, Vedado, Havana, Cuba

Abstract

The goal of this research was to implement a new algorithm for the automatic detection of faults in rolling element bearings, in such a way that it does not depend on the estimation of the shaft rotational speed. The idea was that the algorithm could be applied under variable and unknown rotational speed conditions. The proposed algorithm was based on the detection of phase-relationships between spectral components that emerge when an amplitude modulation appears in the gathered vibration. To do that, a mode decomposition procedure, as well as the Hilbert transform, was applied in order to estimate a detection coefficient, which served as indicator of the presence of the modulation produced by the faults. Lock-in amplifiers were used in order to calculate such an indicator. The effectiveness of the method was validated through experiments preformed by using simulation and real signals. It was proven that the application of the proposed method can lead to an effective detection of the modulation featuring the existence of rolling element bearing faults.

1 Introduction

Different techniques have been developed in order to detect bearing defects. They are based on the application of different techniques, such as signal deconvolution, matching pursuit, spectral coherence, wavelet transform, sparse feature identification, and deep learning, which have proved to be effective under stationary conditions (constant rotational speed of the shafts) [1-5]. If the rotation speed is variable such techniques become in ineffective and more complex algorithms must be applied.

Order tracking has been validated to be one of the most effective tools under varying rotational speed conditions [6]. However, since this method usually requires computing a time-frequency distribution in order to estimate the rotational speed signal, the technique must deal with the time-frequency resolution problem.

An algorithm based on the demodulation of a harmonic of the gear frequency and the subsequent signal resampling was proposed in [7]. In [8], the instantaneous rotational frequency was derived from a time-frequency representation. Other approaches are based on the application of techniques for monocomponent decomposition; for example, in [9], an algorithm was implemented for the phase demodulation of one of the harmonics of the gear frequency when the rotation speed exhibits high variations. In general, a clear understanding about the relationship between the signals resulting from the monocomponent decomposition procedure and the mechanical process that produced them cannot be provided by such methods.

In [10], the rotational speed was estimated from the spectral component given at the rotational frequency or some harmonic of it, that is, the spectral component related to the baseband (unmodulated) rotational speed signal. The existence and order of such harmonic were identified by performing surrogate tests. This procedure requires that the baseband rotational speed signal be given rise at a considerable magnitude, which cannot be always provided.

In [11], the detection of faults in rolling element bearings under nonstationary conditions was proposed to be performed through the estimation of the rotational speed from the vibration produced by gears. This technique required to be implemented on systems with gears.

Then, it is possible to state that the trends of the methods implemented for automatic detection of faults in rolling element bearings under variable rotational speed conditions involve the estimation of the rotational speed. In contrast, this research is aimed to detect some rolling element bearing faults under variable rotational speed conditions without the need of estimating the instantaneous rotational speed. In particular, the faults proposed to be detected are both the inner and the outer race faults.

In this research, Sections 2 and 3 present the model that will be used in order to describe the vibration produced by a local fault in a rolling element bearing. In Section 4, the algorithm proposed to perform the fault detection is exposed. The methodology implemented for algorithm validation is presented in Section 5 and the results obtained are shown and analyzed in Section 6.

2 On the vibration produced by a local fault in a rolling element bearing

When a local fault is running in a rolling bearing, a vibration produced by the impacts of the rolling elements on the fault can excite resonances in the bearing and the machine. By associating the frequency of the impacts with the frequencies of impacts produced by a local fault in each bearing component, not only a bearing condition assessment is achieved but also the identification of the damaged component can be attained. The frequencies of impacts produced by a local fault in each bearing component, called fault characteristic frequencies, can be determined by computing well-known expressions. The fault characteristic frequencies corresponding to both outer race, *BPFO* , and inner race, *BPFI* , of the bearing (these will be the faults to be detected in this research) are:

$$BPFO = \frac{Nb}{2} f_r (1 - \frac{Bd}{Pd} \cos\alpha) \tag{1}$$

$$BPFI = \frac{Nb}{2} f_r (1 + \frac{Bd}{Pd} \cos\alpha) \tag{2}$$

which are function of the rolling element diameter (*Bd*), the mean diameter (*Pd*), the number of rolling elements (*Nb*), the contact angle (α) and the shaft rotation frequency (f_r). Both terms $BPFO/f_r$ and $BPFI/f_r$ are called as *fault characteristic coefficients*.

In this context, the spectrum of the vibration produced when the shaft rotational frequency is constant corresponds to that of an amplitude modulation. Figure 1 shows the theoretical spectrum of the vibration produced by a fault on the outer race: it exhibits spectral components centered at some resonance frequency (f_{res}), which are separated by the fault characteristic frequency (f_{pe}).
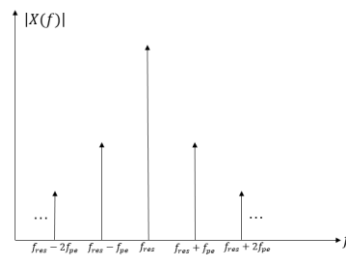

Figure 1: Theoretical spectrum of the vibration produced by a fault on the bearing outer race (constant shaft rotational frequency)

In case of a fault on the inner race, Figure 2 shows the corresponding theoretical spectrum. Similarly to the fault on the outer race, this figure shows spectral components centered at some resonance frequency (f_{res}), which are separated by the fault characteristic frequency (f_{pi}) (see Figure 2). However, in this case an additional amplitude modulation, due to the periodic variation (period equal to $1/f_r$) of the absolute transfer function between the fault and the vibration transducer, arises. As result, the theoretical spectrum shows additional spectral lines separated by the shaft rotational frequency, f_r.

Most of methods for the detection of such faults failures is based on these spectral characteristic. However, if the rotational speed of the shaft is variable, the spectrum characteristic is not longer discrete and the fault detection process turns into a complex task.
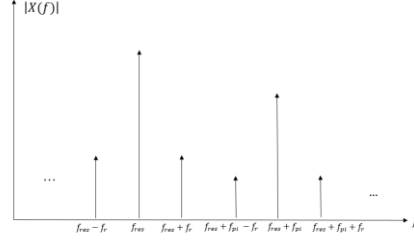

Figure 2: Theoretical spectrum of the vibration produced by a fault on the bearing inner race (constant shaft rotational frequency).

3 Model of the vibration signal produced by a local fault in the rolling element bearing

According to [12], the vibration signal produced by a rolling element bearing under conditions of variable rotational speed, can be expressed by the following model:

$$x(t) = \sum_{i=-\infty}^{+\infty} A_i s(t - T_i) + n(t) \tag{3}$$

where A_i is the amplitude modulation, $s(t)$ depicts the impulse response stimulated by the local defect and $n(t)$ is the noise. The time instant of impulse occurrence is characterized by T_i and calculated as:

$$T_i = \sum_{k=1}^{i} \frac{\theta}{\overline{w}_k} + \Psi_i \tag{4}$$

where the average angular velocity between the k-th and the $(k-1)$-th impulses is given by $\overline{w}_k$, θ is the average angle of occurrence of impulses and Ψ_i is the equivalent jitter in the angular domain.

4 Method proposed for automatic detection of faults in rolling element bearings (unknown and variable rotation speed)

The method proposed for automatic detection of faults in either the outer race or inner race of rolling element bearings, in case of variable and unknown rotational speed of shaft, is based on the detection of the modulation produced whenever the fault runs. Accordingly, the algorithm addresses the detection of the corresponding spectral components. To do that, the product of certain spectral component is averaged in such a way that the result is equal to 0 when the modulation is not produced (there is not phase relationship between the components), that is, no fault is running.

The spectral components that are used in order to detect a fault in the outer race are shown in Figure 3. This figure shows the spectral components of the modulation produced when a fault is running on such a component; these spectral components are given rise at a high frequency band. Besides, an additional spectral component is also shown in the figure and used by the algorithm: the spectral component corresponding to the frequency at which the rolling elements pass over a fixed point on the outer race (f_{pe}). This vibration is produced even though the rolling element bearing geometry is perfect. It is caused by the rotation of a finite number of loaded rolling contacts between the rolling elements and the bearing races [13]. The frequency of this vibration coincides with BPFO.

In this context, the expression that is used in order to detect an outer race fault is:

$$D_o(f_{res}, f_{pe}) = E[X_T(f_{pe})X_T^*(f_{res})X_T(f_{res} + f_{pe})] \tag{5}$$

where $X_T(f)$ is the Fourier transform of $x(t)$, computed for a window of size T.

The spectral components that are used in order to detect a fault in the inner race are shown in Figure 4. Similarly to the previous case, this figure shows, the spectral components of the modulation produced when a fault is running on the inner race. In this case, a low frequency spectral component that is always present, even at very low amplitude, is also used: the spectral component corresponding to the shaft rotational frequency, f_r. Since always there is an unbalanced distribution of residual mass in the shaft that can never be completely removed, this spectral component will always exist [14]. Then, the expression that is used in order to detect an inner race fault is:

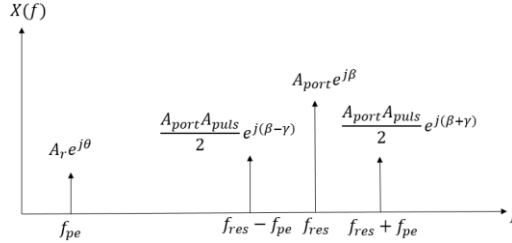$$D_i(f_{res}, f_r) = E[X_T(f_r)X_T(f_{res})X_T^*(f_{res} + f_r)]\tag{6}$$

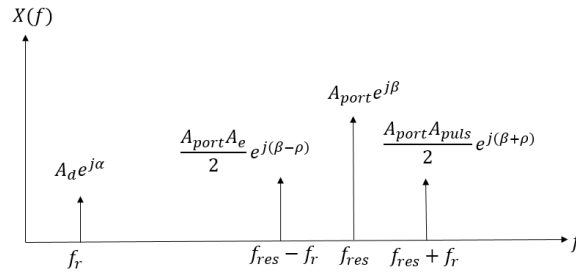Figure 3: Spectral components involved in the detection of an outer race bearing fault.

Figure 4: Spectral components involved in the detection of an inner race bearing fault.

Based on these ideas, Figure 5 depicts a general diagram of the proposed method.

The algorithm is focused to the detection of the modulation, whose carrier frequency, f_c, is equal to the resonance frequency, f_{res}, excited by the fault and whose modulating frequency, f_{mod}, is equal to either the frequency of the pass of the rolling elements by a fixed point on the outer race, f_{pe}, when an outer race fault is running, or the frequency given by the shaft rotation, f_r, when an inner race is running.

In order to carry out the detection procedure, normalized versions of expressions (5) and (6) are proposed to use. The idea of using normalized versions, which derive new coefficients called as *detection coefficients*, was previously presented in [15]. The normalization procedure is performed by the following expression:

$$Norm(E[Z(f_1)Z(f_2)Z(f_3)]) = \left| E\left\{ \frac{Z(f_1)Z(f_2)Z(f_3)}{|Z(f_1)||Z(f_2)||Z(f_3)|} \right\} \right|\tag{7}$$

where $E\{.\}$ is the expected value operator and $Z(f)$ is the value of the spectral component at the frequency f of the analyzed signal. This coefficient takes values between 0 and 1. In case of its application on expressions (5) and (6), the higher the signal-to-noise rate (SNR) of the lying modulation, the closer to 1 the value of the detection coefficient. To calculate the detection coefficient, the vibration signal is split into windows and the value of the spectral components is determined for each window. Then, the values of the detection coefficients, for both the case of an outer race fault (normalized version of expression (5)) and an inner race fault (normalized version of expression (6)), are computed for each window and averaged. High

values (close to 1) of the detection coefficients would be indicating the existence of a fault on the outer race or on the inner race of the bearing.
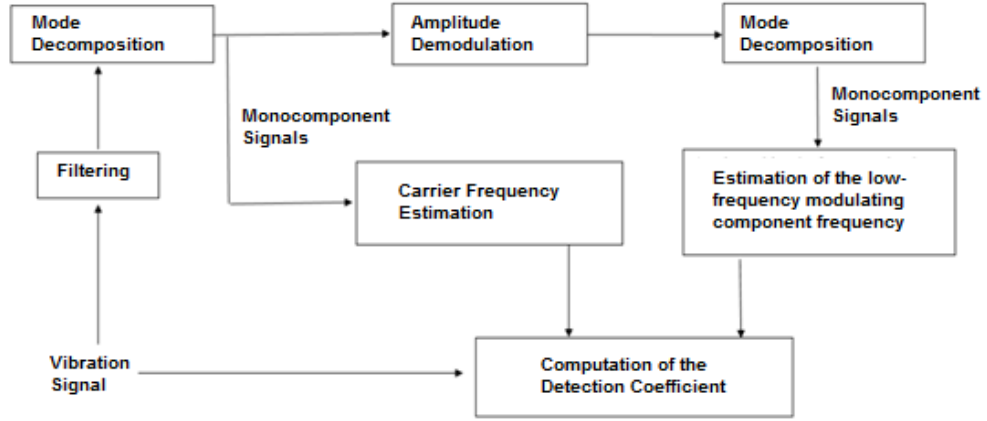

Figure 5: Algorithm for Automatic Detection of both outer and inner race faults

Under variable rotational speed conditions, the Fourier transform cannot be used to obtain the spectral component values. That is why the use of Lock-in amplifiers is proposed, as was performed in [16].

According to the diagram shown in Figure 5, in particular following the top branch, the vibration signal is firstly band pass filtered in order to remove spectral components that do not fall into the spectral band where the modulation must arise in case of bearing fault. This spectral band is a function of the values of the bearing natural frequencies (which can be estimated through modal analysis) and the range of variation of the shaft rotational frequency. The use of such a filter is optional; however it can lead to a more effective result. Subsequently, the decomposition of the vibration signal into monocomponent signals is proposed to do. If a bearing fault exists, it is expected that some achieved monocomponent signal corresponds to the modulation (with carrier frequency equal to the main resonance frequency) produced by the fault. Next, on one hand, the instantaneous frequency of each monocomponent signal, f'_{res_k}, where k is the number of the monocomponent, is obtained by means of the Hilbert transform. And, on the other hand, an amplitude demodulation process is applied to each of the monocomponent signals through the application of the well known Hilbert transform. If the bearing fault exists, some of the demodulated signals will be given at frequency either f_{pe} or f_r, depending on whether the fault is running on the outer race or the inner race, respectively. Then, a second mode decomposition procedure is executed, in this case, on each demodulated signal. If the bearing fault exists, the application of Hilbert transform to each of the obtained demodulated monocomponent signals, in order to estimate their instantaneous frequency, will make the instantaneous frequency either f_{pe} or f_r be achieved. The instantaneous frequency of the monocomponent signal obtained as result of the mode decomposition process performed on the demodulated monocomponent signal k will be denoted as $f'_{p_{kn}}$. Having estimated both f'_{res_k} and $f'_{p_{kn}}$, the detection coefficients corresponding to both outer race and inner race faults can be then determined.

5 Experimental work

Experimental work was carried out through both simulation and real signals. The mode decomposition technique employed in the experiments was the Singular Spectrum Decomposition, SSD, since it has been successfully applied on vibration analysis [17]. The number of monocomponent signals obtained when this technique was applied depended on the threshold selected to stop the decomposition process and the spectrum of the signal in question. In the experiments, a threshold ranging between 0.01 and 0.5 was settled.

5.1 Simulation signals

The simulation signals were built on the basis of the expression (3).
The study cases were:

- No fault (no modulation signal).
- Vibration produced by a fault on the outer race plus vibration produced by the pass of rolling elements on a fixed point of the outer race.
- Vibration produced by a fault on the inner race plus vibration produced by the unbalanced shaft.

A first experiment was performed for the case of constant rotational speed: 30 Hz for the outer race fault signal and 50 Hz for the inner race fault signal. The three signals were sampled at 20 kHz. The fault characteristic coefficient was 5 (for both the outer and inner race fault signals) and the excited resonance frequency was 7 kHz.

A second experiment addressed the algorithm validation under variable rotational speed conditions: increasing from 30 Hz to 40 Hz in case of the outer race fault signal, and increasing from 50 Hz to 60 Hz in case of the inner race fault signal. The outer and inner race fault signals were sampled at 10 kHz and 12 kHz, respectively. The fault characteristic coefficient was 5 and the excited resonance frequency was 2 kHz.

For both groups of signals, the bandpass filter employed at the algorithm beginning was set to be centered at the resonance frequency and to have a bandwidth equal to 2 kHz.

White Gaussian noise was added to signals in order to validate the algorithm for different SNRs, in this case, 10 dB and 20 dB. Then, the implementation of a statistical analysis could be performed.

5.2 True signals

The true signals used in this work corresponded to outer and inner race fault signals, and no-fault signals as well, for constant and variable rotational speed conditions.

A first experiment (for the tests under constant rotational speed conditions) was performed by using signals available at [18], which is an online maintenance failure database. Two signals corresponding to an outer race fault and two signals corresponding to an inner race fault were used. The shaft rotational speed was   25 Hz and the signals were sampled at 48828 Hz for 3 s. Besides, two signals corresponding to no-fault signals were also used. In this case, the shaft rotational speed was 25 Hz and the signals were sampled at 97655 Hz for 6 s. Since, this sampling frequency is twice the sampling frequency applied to fault signals, a subsampling procedure was implemented. As result, no-fault signals sampled at 48828 Hz for 3 s were obtained. The most significant band occupied by the resonances excited by the bearing faults was found around 4 kHz. Then, for these signals the bandpass filter employed at the algorithm beginning was set to be centered at 4 kHz; the bandwidth was set to be 6 kHz.

A second experiment (for the tests under variable rotational speed conditions) was done through signals available at [19], which is an online web site that includes signals acquired from a SpectraQuest (MFS-PK5M) Fault Simulator. The available data includes vibration signals collected under different rolling element bearing conditions. The signals were sampled at 200 kHz for 10 s. Signals having the characteristics presented in Table 1 [19] were used.

Operating conditions	Shaft rotational speed	Fault characteristic coefficient
Normal condition	HA-2 (speed increasing from 14.1 Hz to 29.0 Hz)	No-fault signal
Outer race fault	OA-1 (speed increasing from 14.8 Hz a 21.1 Hz)	3,57
Inner race fault	IA-1 (speed increasing from 12.5 Hz to 27.8 Hz)	5,43

Table 1: Characteristics of true signals from [19].

This dataset of signals was subsampled to obtain new signals sampled at 50 kHz. In this case, the band occupied by the most significant excited resonance frequencies was found around 1 kHz. Then, for such signals, the bandpass filter used at the algorithm beginning was set to be centered at 1 kHz; the bandwidth was set to be 1 kHz. At this point, it is necessary to mention that for the no-fault signals available at [18] and [19] the spectral analysis revealed that certain modulation patterns are present in the signals (see Figure 6). Since this is not meaning that there is a fault in the bearing, this feature could affect the success of the algorithm application, mainly when the frequencies of the involved spectral components are close.
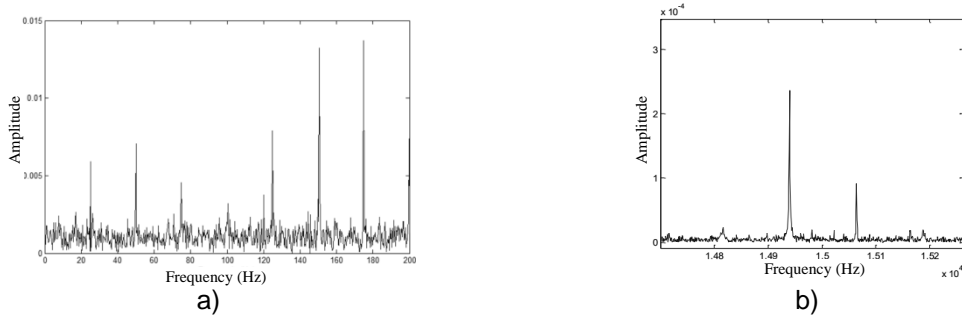
Figure 6. Example of the modulation pattern that appears in a) no-fault signals available at [18] and b) no-fault signals available at [19].

6   Working with simulation signals

Experimental work was carried out through both simulation and real signals. The mode decomposition

The result of the work with simulation signals is presented. It should be recalled that 20 realizations of signals, per condition (no fault, outer race fault and inner race fault) and SNR (10 dB and 20 dB), were simulated.

However, it should be realized that the noise can make the detection coefficient take either high values when the condition simulated corresponds to no-fault state or low values when the condition simulated corresponds to the faulty bearing. This could be due to the limitations of the SSD technique to deal with signals with low SNR. That is why the indicator more convenient to follow is the frequency at which the detection coefficient takes high values rather than a singular value of this coefficient by itself.

In this work, the detection coefficient is regarded as high when it takes values higher than 0,7. This threshold was empirically settled as result of the analysis of the signals under study. However, it can be higher or lower which will yield results some different (but corresponding) to those presented in this work.

The results of the first experiment, performed for the case of constant rotational speed, are presented in tables 2 and 3. Tables 2 and 3 show the frequency (percentage) at which high values (higher than 0,7) of the corresponding detection coefficient are obtained, for SNR = 10 dB and SNR = 20 dB, respectively. These tables reveal that the highest percentages of high values of the detection coefficient are achieved when a fault is running. For SNR = 20 dB, the percentages of high values of the detection coefficient, in case of both outer and inner race faults were running, were about twice the percentage of high values of the detection coefficient achieved when the no-fault condition was simulated. This result was similar to that achieved for SNR = 10 dB. The fact that the SNR degradation did not affect significantly the performance of the algorithm is very noticeable.

Percentage of the number of times that high values (higher than 0,7) of the corresponding detection coefficient are obtained for a particular bearing condition	Outer race fault. (Percentage of high values of the detection coefficient given by the normalized version of expression (5))	14,7 %
	Inner race fault. (Percentage of high values of the detection coefficient given by the normalized version of expression (6))	16,5 %
	No-fault (Percentage of high values of the detection coefficients given by the normalized versions of expressions (5) and (6). Both coefficients are computed per window; if at least one of them is high, one high value of coefficient is involved in the percentage computation)	8,3 %

Table 2: Results obtained from the computation of the detection coefficients in case of simulation signals (under constant rotational speed conditions). SNR = 20 dB.

Percentage of the number of times that high values (higher than 0,7) of the corresponding detection coefficient are obtained for a particular bearing condition.	Outer race fault. (Percentage of high values of the detection coefficient given by the normalized version of expression (5))	15,5 %
	Inner race fault. (Percentage of high values of the detection coefficient given by the normalized version of expression (6))	15,8 %
	No-fault (Percentage of high values of the detection coefficients given by the normalized versions of expressions (5) and (6). Both coefficients are computed per window; if at least one of them is high, one high value of coefficient is involved in the percentage computation)	7,7 %

Table 3: Results obtained from the computation of the detection coefficients in case of simulation signals (under constant rotational speed conditions). SNR = 10 dB.

The results of the second experiment, performed for the case of variable rotational speed, are presented in tables 4 and 5. These tables show results very similar to those obtained in case of constant rotational speed. Indeed, such tables confirm that the highest percentages of high values of the detection coefficient are achieved when a fault is running. For SNR = 20 dB, the percentage of high values of the detection coefficient, in case of outer and inner race faults, were about 2 and 3 times the percentage of high values achieved under no-fault conditions, respectively. For SNR = 10 dB, the percentages of high values of the detection coefficient, in case of outer and inner race faults, were 1,85 and 1,36 times the percentage of high values achieved under no-fault conditions, respectively. In this experiment is visible the performance degradation due to noise.

Percentage of the number of times that high values (higher than 0,7) of the corresponding detection coefficient are obtained for a particular bearing condition	Outer race fault. (Percentage of high values of the detection coefficient given by the normalized version of expression (5))	26,7 %
	Inner race fault. (Percentage of high values of the detection coefficient given by the normalized version of expression (6))	41,3 %
	No-fault (Percentage of high values of the detection coefficients given by the normalized versions of expressions (5) and (6). Both coefficients are computed per window; if at least one of them is high, one high value of coefficient is involved in the percentage computation)	13,9 %

Table 4: Results obtained from the computation of the detection coefficients in case of simulation signals (under variable rotational speed conditions). SNR = 20 dB.

Percentage of the number of times that high values (higher than 0.7) of the corresponding detection coefficient are obtained for a particular bearing condition	Outer race fault. (Percentage of high values of the detection coefficient given by the normalized version of expression (5))	25,2 %
	Inner race fault. (Percentage of high values of the detection coefficient given by the normalized version of expression (6))	18,5 %
	No-fault (Percentage of high values of the detection coefficients given by the normalized versions of expressions (5) and (6). Both coefficients are computed per window; if at least one of them is high, one high value of coefficient is involved in the percentage computation)	13,6 %

Table 5: Results obtained from the computation of the detection coefficients in case of simulation signals (under variable rotational speed conditions). SNR = 10 dB.

7 Working with true signals

The results of working with real signals are shown in this Section.

For the first experiment (involving vibration signals gathered under constant rotational speed conditions), table 6 presents the results obtained from the application of the proposed algorithm. This table confirms that the highest percentages of high values of the detection coefficient are achieved when a bearing fault is running. For the signals under study, the percentage of high values of the detection coefficient, in case of outer and inner race faults, were about 3,2 and 2,2 times the percentage of high values achieved under no-fault conditions, respectively.

Percentage of the number of times that high values (higher than 0,7) of the corresponding detection coefficient are obtained for a particular bearing condition	Outer race fault. (Percentage of high values of the detection coefficient given by the normalized version of expression (5))	71,4 %
	Inner race fault. (Percentage of high values of the detection coefficient given by the normalized version of expression (6))	50,0 %
	No-fault (Percentage of high values of the detection coefficients given by the normalized versions of expressions (5) and (6). Both coefficients are computed per window; if at least one of them is high, one high value of coefficient is involved in the percentage computation)	22,2 %

Table 6: Results obtained from the computation of the detection coefficients in case of real signals (under constant rotational speed conditions).

For the second experiment (involving vibration signals gathered under variable rotational speed conditions), table 7 presents the obtained results. Once again, the fact that the highest percentages of high values of the detection coefficient are achieved when the fault is running is confirmed. However, for this dataset, the mode decomposition technique (i.e., SSD) was not able to deliver any monocomponent in case of the signals acquired under no-fault conditions. In the context of the algorithm, this means that no modulation appears in such signals and therefore there is not bearing fault.

Percentage of the number of times that high values (higher than 0,7) of the corresponding detection coefficient are obtained for a particular bearing condition	Outer race fault. (Percentage of high values of the detection coefficient given by the normalized version of expression (5))	15,4 %
	Inner race fault. (Percentage of high values of the detection coefficient given by the normalized version of expression (6))	44,4 %
	No-fault (Percentage of high values of the detection coefficients given by the normalized versions of expressions (5) and (6). Both coefficients are computed per window; if at least one of them is high, one high value of coefficient is involved in the percentage computation)	0 %

Table 7: Results obtained from the computation of the detection coefficients in case of real signals (under variable rotational speed conditions).

8 Acknowledgments

9 Conclusions

In this research, a new method for the automatic detection of fault in roller bearing, in particular both outer and inner race faults, under variable and unknown rotational speed conditions was implemented and validated. The novelty of this proposal resides in that it also takes into account the presence of low frequency vibrations that are always present and are phase-related with the high frequency spectral components (modulation) produced when bearing faults are running.

By the work with simulation and real signals, it was proven that the application of the proposed method can lead to an effective detection of the modulation featuring the existence of rolling element bearing faults. Although high values of the detection coefficients could indicate the presence of such a modulation, this coefficient by itself is not enough to conclude that a fault is running. A more robust indicator in this case is the frequency at which high values the detection coefficient is given. That is, as this frequency gets higher, the existence of the fault will be more likely. Thus, this indicator must be considered as a relative indicator, rather than an absolute indicator, since it is more suitable to be applied on a trend analysis.

10 References

[1] Wang Z, Du W, Wang J, et al. Research and application of improved adaptive MOMEDA fault diagnosis method. Measurement. 2019;140:63-75.

[2] Qin Y, Zou J, Tang B, et al. Transient feature extraction by the improved orthogonal matching pursuit and K-SVD algorithm with adaptive transient dictionary. IEEE Transactions on Industrial Informatics. 2020;16(1):215 - 227.

[3] Wang D, Zhao X, Kou L, et al. A simple and fast guideline for generating enhaced/squared envelope spectra from spectral coherence for bearning fault diagnosis. Mechanical Systems and Signal Processing. 2019;122:754-768.

[4] Quin Y. A new family of model-based impulsive wavelets and their sparse representation for rolling bearning fault diagnosis. IEEE Transactions on Industrial Electronics. 2017;65(3):2716-2726.

[5] Guo L, Lei Y, Xing S, et al. Deep convolutional transfer learning network: A new method for intelligent fault diagnosis of machines with unlabeled data. IEEE Transactions on Industrial Electronics. 2018;66(9):7316-7325.

[6] Wang Y, Tse P, Tang B, et al. Order spectrogram visualization for rolling bearing fault detection under speed variation conditions. Mechanical Systems and Signal Processing. 2019;122:580–596.

[7] Bonnardot F, ElBadaoui M, Randall RB, et al. Use of the acceleration signal of a gearbox in order to perform angular resampling(with limited speed fluctuation), Mechanical Systems and Signal Processing. 2005;19(4):766-785.

[8] Urbanek J, Barszcz T, Antoni J. A two-step procedure for estimation of instantanous rotational speed with large fluctuations. Mechanical Systems and Signal Processing. 2013;38(1):96-102.

 [9] Zhao M, Lin J, Wang X, et al. A tacho-less order tracking technique for large speed variations. Mechanical Systems and Signal Processing. 2013;40(1):76-90.

[10] Wang Y, Tang B, Qin Y, et al. Rolling Bearning Fault Detection of Civil Aircraft Engine based on Adaptive Estimation of Instantaneous Angular Speed. IEEE Transactions on Industrial Informatics. 2020;16(7):4938-4948.

[11] Rodriguez A, Hernandez F, Ruiz M. Automatic detection of Rolling Element Bearning Faults to Be Applied on Mechanical Systems Comprised by Gears. In Nonstationary Systems:Theory and Applications. Switzerland: Springer Nature; 2021. DOI 10.1007/978-3-030-82110-4_12.

[12] Borghesani P, Ricci R, Chatterton S, et al. A new procedure for using envelope analysis for rolling element bearing diagnostics in variable operating conditions. Mechanical Systems and Signal Processing. 2013;38(1):23-35.

[13] Stolarski T. Tribology in Machine Design, Springer, Butterworth-Heinemann, 1999. [Cited on November 11th, 2022]. Available at https://www.sciencedirect.com/book/9780080519678/tribology-in-machine-design.

[14] Adams ML. Rotating Machinery Vibration. From Analysis to Troubleshooting, US: Taylor and Francis Group LLC, 2010.

[15] Hernandéz F, Iturrospe A. Direct analysis of non-quadratic phase coupling for detection of linearly modulated signals. In: Annual Conference of the Prognostics and Health Management Society, California,USA; 2015 [Cited on November 11th, 2022]. Available at https://papers.phmsociety.org/index.php/ phmconf/article/view/2714.

[16] Ruiz ML, Hernandez F, Gómez J, et al. Application of Lock Amplifier on gear diagnosis. Measurement. 2017;107:120-127.

[17] Calzadilla A, Catalá A, Hernández F, et al. Assessing the monocomponent decomposition technique able to more accurately deliver the vibration produced by a gear. Journal of Applied Research and Technology. 2020;18(3):101-107.

[18] Bechhoefer E, Condition Based Maintenance Fault Database for Testing of Diagnostic and Prognostics Algorithms. Data Assambled and Prepared on behalf of MFPT Vibration Institute. 2021. [Cited on November 11th, 2022]. Available at https://www.mfpt.org/fault-data-sets/

[19] Huang H, Baddour N. Bearing Vibration Data under Time-varying Rotational Speed Conditions. Mendeley Data. 2019;21:1745-1749.